IEEE Access
Multidisciplinary | Rapid Review | Open Access Journal

Received November 22, 2018, accepted December 2, 2018, date of publication December 5, 2018,
date of current version December 31, 2018.

Digital Object Identifier 10.1109/ACCESS.2018.2885082

Practical Adaptive Integral Terminal Sliding Mode Control for Cable-Driven Manipulators

YAOYAO WANG [1,2], (Member, IEEE), FEI YAN [1], KANGWU ZHU [3], BAI CHEN [1], AND HONGTAO WU [1]

[1]College of Mechanical and Electrical Engineering, Nanjing University of Aeronautics and Astronautics, Nanjing 210016, China
[2]State Key Laboratory of Fluid Power and Mechatronic Systems, Zhejiang University, Hangzhou 310027, China
[3]Shanghai Institute of Spaceflight Control Technology, Shanghai 200233, China

Corresponding author: Yaoyao Wang (yywang_cmee@nuaa.edu.cn)

This work was supported in part by the National Natural Science Foundation of China under Grant 51705243, in part by the Natural Science Foundation of Jiangsu Province under Grant BK20170789, in part by the Open Foundation of the State Key Laboratory of Fluid Power and Mechatronic Systems under Grant GZKF-201606, and in part by the China Postdoctoral Science Foundation under Grant 2018M630552.

ABSTRACT To guarantee high-performance tracking control of cable-driven manipulators under complex lumped uncertainties, we propose a novel practical adaptive integral terminal sliding mode (AITSM) control scheme in this paper. The proposed control scheme utilizes time-delay estimation (TDE) to estimate and compensate the system dynamics and therefore ensures an attractive model-free control structure. Meanwhile, a novel adaptive algorithm is designed to timely and appropriately update the gains for the AITSM manifold and combined adaptive reaching law (ARL). High control accuracy, fast dynamical response, and strong robustness can be effectively ensured, thanks to the proposed AITSM manifold and combined ARL. The stability of the closed-loop control system is analyzed using the Lyapunov stability theory. Comparative experiments were conducted, and the corresponding results show that the newly proposed TDE-based AITSM control scheme can provide a better and comprehensive control performance than the existing AITSM control method.

INDEX TERMS Model-free, time-delay estimation (TDE), adaptive integral terminal sliding mode (AITSM), cable- driven manipulators, tracking control.

I. INTRODUCTION

For the past few decades, robot manipulators have been broadly utilized in lots of practical applications. Thanks to the high stiffness and simple structure, they can easily conduct complex automatic tasks with high precision and fast dynamical response [1]–[6]. But it is usually not safe for human to work around them with physical interactions due to their large moving inertial and high stiffness. To effectively settle above issues and ensure safe interactions with human, scholars and engineers developed the cable-driven manipulators [7], [8]. The main idea of cable-driven manipulators is to move the drive units from the joints to base and realize force/motion transmission through cable. Benefitting from above arrangement, the cable-driven manipulators can provide smaller moving inertial, better flexibility and safety for physical interactions with human [9]–[12]. However, the utilization of cable-driven technique will also lead to extra difficulties for accurate control of cable-driven manipulators, such as low stiffness, complex dynamics and external disturbance [13], [14].

As one of the most important discoveries in the modern control theory, sliding mode (SM) control can effectively handle aforesaid difficulties [15]–[21]. SM control has a simple structure and can provide strong robustness for complex applications, such as robot manipulators [22], [23], underwater robots [24]–[26], legged walking robots [27], cable-driven systems [28], [29]. SM control has been greatly improved since it was proposed and good control performance can be effectively ensured [17]–[29]. In the meantime, it has also been widely proved that finite-time convergence may lead to high-precision performance and fast dynamical response [30]–[32]. Thus, several improved SM schemes, such as terminal SM (TSM), fast TSM (FTSM), nonsingular TSM (NTSM) and FTSM (NFTSM) have been proposed and studied [30]–[37]. By introducing a nonlinear term into the linear SM manifold, the TSM and FTSM manifolds can provide finite time convergence. Thus, better comprehensive performance will be obtained with the TSM and FTSM control. However, TSM and FTSM have singularity issue which may obviously degrade the control performance.

Therefore, the NTSM and NFTSM control schemes have been proposed [25]–[27]. Although above control methods have achieved good results, it is still not easy to use them under complicated practical situations considering the utilization of dynamic model or complex approximation schemes.

To effectively solve above issues, the time-delay estimation (TDE) technique was proposed and applied [38]–[40]. By using the time-delayed states of the system to estimate its own current lumped dynamics, TDE technique can bring a fascinating model-free control scheme [41]–[44]. Hence, TDE technique has been widely applied for lots of systems since it was proposed, such as underwater robots [41]–[43], robot manipulators [44]–[48], humanoid robots [49], and lower limb exoskeleton [50], [51]. The utilization of TDE will lead to inevitable estimation errors especially when systems contain fast-varying dynamics. Therefore, the TDE technique is usually used as framework to enjoy its model-free advantage; meanwhile, other robust control schemes are cooperated to further enhance the control performance under complex practical applications. The obtained control schemes can naturally enjoy advantages from both TDE technique and adopted robust control schemes.

Recently, a novel adaptive integral TSM (AITSM) control was proposed for the control of upper limb exoskeletons [52]. The proposed control scheme contains two parts, i.e. the dynamic model part and the AITSM control part. The former is used to compensate the known system dynamics, while the latter is applied to ensure high performance control under complicated situations. The proposed control scheme requires no boundary information of the lumped uncertainties thanks to the features of adaptive law [53]-[55]. In the meantime, the control performance has also been effectively enhanced benefitting from the advantages of ITSM scheme [56]–[60]. Although the control scheme from [52] has obtained some exciting theoretical and experimental results, it still has three aspects to improve: *1)* the proposed control scheme requires system dynamic model, which can be very difficult to obtain for complex systems, such as cable-driven manipulators; *2)* the proposed adaptive algorithm is*monotonically increasing*, which may lead to inappropriately large gain for the robust term and then cause serious chatters and even substantial damage to the system hardware. *3)* the designed ITSM manifold still uses constant gain and may result in control performance degradation when large uncertainties appear.

In this work, the aforesaid issues have been effectively addressed based on the existing ITSM control [52], [56]–[60]. A novel TDE-based AITSM control is proposed and studied. The proposed control scheme mainly contains three parts, i.e. TDE part, AITSM manifold part and combined adaptive reaching law (ARL) part. The TDE is applied to estimate the lumped system dynamics and ensures a model-free control scheme. In the meantime, the AITSM manifold and combined ARL are used to enhance the control performance using a properly designed adaptive algorithm. The proposed control scheme requires no dynamic model and therefore can be easily utilized for complex practical applications thanks to TDE. Meanwhile, high-precision control and fast dynamical response can also be guaranteed benefitting from the proposed AITSM control scheme. The stability of control system is proved using Lyapunov theory. Finally, comparative experiments have been performed to demonstrate the effectiveness and advantages of our newly proposed control scheme over the existing one.

The contributions of this work are:

1) to propose a novel AITSM manifold, which uses an adaptive algorithm to properly generate the gain based on the control errors;
2) to propose a novel TDE-based control using above AITSM manifold and a combined ARL; and
3) to prove the stability of the control system considering the designed adaptive dynamics.

The remainder is organized as follows. Section II presents the problem description briefly, and then Section III gives the proposed control scheme design and some discussions. Comparative experimental results are presented and analyzed in Section IV. Finally, Section V concludes this paper.

II. PROBLEM DESCRIPTION

The cable-driven manipulators can be described using the following equations [9], [10]

$$\mathbf{I}\ddot{\boldsymbol{\phi}} + \mathbf{d}_m\dot{\boldsymbol{\phi}} = \boldsymbol{\tau} - \boldsymbol{\tau}_s \quad (1)$$

$$\mathbf{m}(\mathbf{q})\ddot{\mathbf{q}} + \mathbf{c}(\mathbf{q}, \dot{\mathbf{q}})\dot{\mathbf{q}} + \mathbf{g}(\mathbf{q}) + \mathbf{f}(\mathbf{q}, \dot{\mathbf{q}}) = \boldsymbol{\tau}_s - \boldsymbol{\tau}_d \quad (2)$$

$$\mathbf{k}_p(\boldsymbol{\phi} - \mathbf{q}) + \mathbf{k}_d\left(\dot{\boldsymbol{\phi}} - \dot{\mathbf{q}}\right) = \boldsymbol{\tau}_s \quad (3)$$

where $\mathbf{I}$ and $\mathbf{d}_m$ stand for the inertia and damping matrices of the motors, $\boldsymbol{\phi}$ and $\mathbf{q}$ are the position vectors of the motors and joints. $\boldsymbol{\tau}_s$ and $\boldsymbol{\tau}$ represent the torques generated by the joint compliance and motors. $\mathbf{m}(\mathbf{q})$ stands for the inertia matrix, while $\mathbf{c}(\mathbf{q}, \dot{\mathbf{q}})$ is the Coriolis/centrifugal matrix, $\mathbf{g}(\mathbf{q})$ represents the gravitational vector, $\mathbf{f}(\mathbf{q}, \dot{\mathbf{q}})$ stands for the friction vector. $\boldsymbol{\tau}_d$ is the lumped disturbance, $\mathbf{k}_p$ and $\mathbf{k}_d$ stand for the stiffness and damping matrices of the joints.

Substituting (2) into (1) and bringing in a constant parameter $\bar{\mathbf{m}}$, we have the following integrated dynamics

$$\bar{\mathbf{m}}\ddot{\mathbf{q}} + \mathbf{w} = \boldsymbol{\tau} \quad (4)$$

where $\mathbf{w}$ stands for the remaining dynamics and is given as

$$\mathbf{w} = (\mathbf{m}(\mathbf{q}) - \bar{\mathbf{m}})\ddot{\mathbf{q}} + \mathbf{c}(\mathbf{q}, \dot{\mathbf{q}})\dot{\mathbf{q}} + \mathbf{g}(\mathbf{q}) + \mathbf{f}(\mathbf{q}, \dot{\mathbf{q}}) + \mathbf{I}\ddot{\boldsymbol{\phi}} + \mathbf{d}_m\dot{\boldsymbol{\phi}} + \boldsymbol{\tau}_d \quad (5)$$

Note that $\mathbf{w}$ is extremely complicated and can be very difficult to achieve with conventional methods.

Therefore, the motivation of this paper can be described as follows: for a given reference trajectory $\mathbf{q}_d$, design a proper and effective control $\boldsymbol{\tau}$ such that the cable-driven manipulators can accurately track $\mathbf{q}_d$. Additionally, the control $\boldsymbol{\tau}$ should also be *simple* and *easy* to use in complex practical applications.

III. PROPOSED AITSM CONTROL SCHEME USING TDE

In this section, we propose a novel AITSM control scheme using TDE technique. The newly proposed control scheme contains three main parts, i.e. the TDE, AITSM manifold and combined ARL. The TDE scheme is applied to obtain the estimation of system dynamics in a simple way, meanwhile the AITSM manifold and combined ARL are utilized to ensure satisfactory control performance with an adaptive algorithm.

A. PROPOSED AITSM CONTROL

Define the control error as $\mathbf{e} = \mathbf{q}_d - \mathbf{q}$. Then, to guarantee high control accuracy and fast dynamical response, we propose the following AITSM manifold as

$$\mathbf{s} = \dot{\mathbf{e}} + \hat{\mathbf{k}} \int_0^t \left(\boldsymbol{\alpha}\mathbf{sig}\left(\dot{\mathbf{e}}\right)^{\gamma_1} + \boldsymbol{\beta}\mathbf{sig}\left(\mathbf{e}\right)^{\gamma_2}\right)\mathbf{d}t \tag{6}$$

where $\boldsymbol{\alpha}$ and $\boldsymbol{\beta}$ are diagonal matrices with positive elements, $0 < \gamma_1 < 1$ and $\gamma_2 = \gamma_1/(2-\gamma_1)$, $\hat{\mathbf{k}}$ is a positive adaptive gain which will be given later. For concision, the following notations $\mathbf{sig}\left(\dot{\mathbf{e}}\right)^{\gamma_1} = \left[sig\left(\dot{e}_1\right)^{\gamma_1}, \ldots, sig\left(\dot{e}_n\right)^{\gamma_1}\right]$, $sig\left(e_1\right)^{\alpha_{11}} = |e_1|^{\alpha_{11}} \operatorname{sgn}\left(e_1\right)$ are utilized here and $\operatorname{sgn}(x)$ is given mathematically as

$$\operatorname{sgn}\left(x\right) = \begin{cases} 1, & \text{if } x > 0 \\ 0, & \text{if } x = 0 \\ -1, & \text{if } x < 0 \end{cases} \tag{7}$$

Usually, the gain $\mathbf{k}$ for ITSM manifold is a pre-selected constant [52]. However, it can be very difficult or laborious to obtain a proper gain under complex lumped uncertainties. If the gain $\mathbf{k}$ is selected inappropriately small, the control performance will degrade when large uncertainties appear. Contrarily, if the gain $\mathbf{k}$ is tuned inappropriately large, the noise effect may be aroused under large uncertainties. Thus, we try to enhance the control performance with an adaptive gain $\hat{\mathbf{k}}$. When the control performance tends to degrade, the gain $\hat{\mathbf{k}}$ will increase accordingly to provide extra robustness and guarantee good control performance under lumped uncertainties. When the control performance is good, the gain $\hat{\mathbf{k}}$ will decrease to suppress the potential noise effect and ensure good dynamical performance.

Afterwards, the following combined ARL is applied to provide satisfactory comprehensive control performance as

$$\dot{\mathbf{s}} = -\boldsymbol{\rho}_1\mathbf{s} - \boldsymbol{\rho}_2\mathbf{sig}\left(\mathbf{s}\right)^{\lambda} - \hat{\boldsymbol{\rho}}_3\mathbf{sgn}\left(\mathbf{s}\right) \tag{8}$$

where $\boldsymbol{\rho}_1$, $\boldsymbol{\rho}_2$ are positive constant gains, while $\hat{\boldsymbol{\rho}}_3$ is an adaptive gain to be designed and λ is positive gain satisfying $0 < \lambda < 1$.

As shown in (8), the utilized ARL has two parts. The first part is the fast-TSM-type (FTSM) RL [32], the other part is the element $\hat{\boldsymbol{\rho}}_3\mathbf{sgn}\left(\mathbf{s}\right)$. The former is utilized to ensure high control accuracy and fast dynamical response, while the latter is used to provide extra strong robustness against time-varying lumped disturbance with adaptive gain.

To further enhance the control performance, we use the following adaptive algorithm for the proposed AITSM manifold and combined ARL [47]

$$\dot{\theta}_i = \begin{cases} \mu_{1i}\left|s_i\right| \operatorname{sgn}\left(\theta_{i\_\mathrm{mid}} - \theta_i\right), & \text{if } \theta_i \geq \theta_{i\_\max} \text{ or } \theta_i \leq 0 \\ \mu_{1i}\left|s_i\right|, & \text{if } 0 < \theta_i < \theta_{i\_\max}, \\ & \quad \left|s_i\right| > \Delta_i \\ -\mu_{2i}\left|s_i\right|, & \text{if } 0 < \theta_i < \theta_{i\_\max}, \\ & \quad \left|s_i\right| \leq \Delta_i \end{cases} \tag{9}$$

$$\hat{k}_{ii} = k_{1i}\left(1 + k_{2i}\theta_i\right), \quad \hat{\rho}_{3ii} = k_{3i}\left(1 + k_{4i}\theta_i\right) \tag{10}$$

where $\mu_{1i}, \mu_{2i}, \Delta_i, k_{1i}, k_{2i}, k_{3i}, k_{4i}$ are positive parameters and $\mu_{2i} > \mu_{1i}$, while $\theta_{i\_\max}$ is a constant parameter to describe the maximum value of θ_i, and $\theta_{i\_\mathrm{mid}} = \theta_{i\_\max}/2$. It is obvious that the adaptive gain θ_i is bounded within $\theta_i \epsilon [0, \theta_{i\_\max}]$.

Taking the adaptive algorithm (9) to analyze, we can see that when the control accuracy is relative low, i.e. $|s_i| > \Delta$, the adaptive gain θ_i will increase to enhance the control performance. On the other hand, if the control accuracy is good, i.e. $|s_i| \leq \Delta$, the θ_i will decrease rapidly to ease the noise effect and obtain relative smooth performance. In the mean-time, there are two designed speeds as given in (9), which can be written as $\mu_{1i}|s_i|$ and $\mu_{2i}|s_i|$. The speed $\mu_{1i}|s_i|$ is used for all situations except that the control accuracy is good and the adaptive gain θ_i needs to be reduced. Under this situation, the sliding variable $|s_i|$ is actually quite small, and the speed $\mu_{1i}|s_i|$ will be improperly small and may lead to inappropriately large gain θ_i. Thus, the speed $\mu_{2i}|s_i|$ is utilize to rapidly reduce the gain θ_i considering $\mu_{2i} > \mu_{1i}$ and then ensure smooth control performance.

Using the proposed AITSM manifold (6), combined ARL (8) and the adaptive law (9)(10), we design the following AITSM control scheme as

$$\begin{aligned} \boldsymbol{\tau} &= \bar{\mathbf{m}}\mathbf{u} + \hat{\mathbf{w}} \\ \mathbf{u} &= \ddot{\mathbf{q}}_d + \boldsymbol{\psi}\left(\mathbf{e}, \hat{\mathbf{k}}\right) + \boldsymbol{\rho}_1\mathbf{s} + \boldsymbol{\rho}_2\mathbf{sig}\left(\mathbf{s}\right)^{\lambda} + \hat{\boldsymbol{\rho}}_3\mathbf{sgn}\left(\mathbf{s}\right) \end{aligned} \tag{11}$$

$$\begin{aligned} \boldsymbol{\psi}\left(\mathbf{e}, \hat{\mathbf{k}}\right) &= \hat{\mathbf{k}}\boldsymbol{\alpha}\mathbf{sig}\left(\dot{\mathbf{e}}\right)^{\gamma_1} + \hat{\mathbf{k}}\boldsymbol{\beta}\mathbf{sig}\left(\mathbf{e}\right)^{\gamma_2} \\ &\quad + \dot{\hat{\mathbf{k}}} \int_0^t \left(\boldsymbol{\alpha}\mathbf{sig}\left(\dot{\mathbf{e}}\right)^{\gamma_1} + \boldsymbol{\beta}\mathbf{sig}\left(\mathbf{e}\right)^{\gamma_2}\right)\mathbf{d}t \end{aligned} \tag{12}$$

where $\hat{\mathbf{w}}$ stands for the estimation of the remaining system dynamics. It is obvious that if we can obtain $\hat{\mathbf{w}}$ accurately and properly, the control problem will be easily solved with above AITSM control scheme. However, as we explain aforesaid, the remaining dynamics $\mathbf{w}$ is very complex and can be difficult or laborious to obtain.

B. TIME-DELAY ESTIMATION TECHNIQUE

To solve above issue, we apply the TDE technique in this subsection. The TDE scheme is a fascinating estimation algorithm, which can obtain the system dynamics in a simple but effect way. More importantly, TDE scheme is model-free and requires no system dynamic information. Mathematically, the TDE scheme can be written in the following equation as

$$\hat{\mathbf{w}}\left(t\right) = \mathbf{w}\left(t - \eta\right) \tag{13}$$

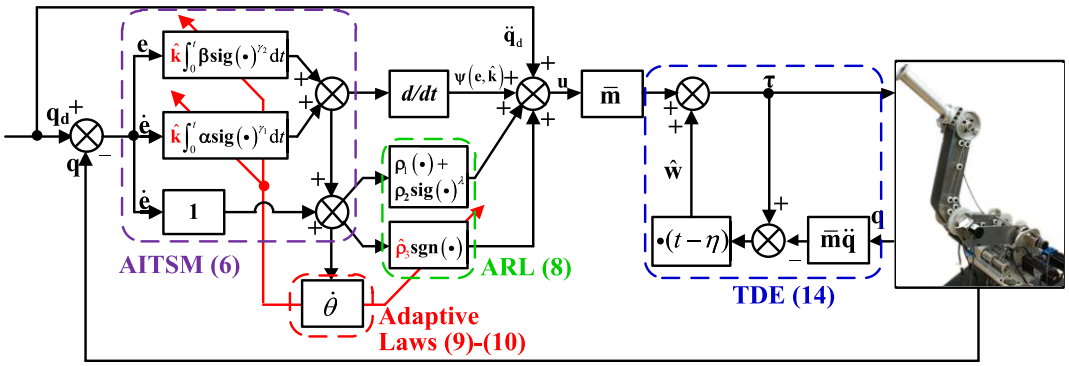

FIGURE 1. The block diagram of our newly proposed TDE-based AITSM control scheme.

As indicated in (13), the main idea of TDE scheme is to use the time-delayed value of the system dynamics to estimate its own current value. For most practical systems, such as robotic manipulators, above equation can be very effective using efficiently small delayed time η. Taking the dynamics of cable-driven manipulators into consideration, we can see that the TDE technique has also effectively handled the flexibility described by (3) together with other unknown lumped dynamics. This is a very attractive feature since the flexibility is usually quite hard to obtain using traditional methods.

Afterwards, combining (13) with (4), we have

$$\hat{\mathbf{w}}(t) = \mathbf{w}(t-\eta) = \boldsymbol{\tau}(t-\eta) - \bar{\mathbf{m}}\ddot{\mathbf{q}}(t-\eta) \tag{14}$$

Finally, we can see from (14) that all the signals required by TDE scheme are the time-delayed control torque and acceleration signals. The $\boldsymbol{\tau}(t-\eta)$ is obtained with the time- delayed of $\boldsymbol{\tau}$, while $\ddot{\mathbf{q}}(t-\eta)$ is obtained using numerical differentiation $\ddot{q}(t-\eta) = (q(t) - 2q(t-\eta) + q(t-2\eta))/\eta^2$. In the meantime, the numerical differentiation will inevitably enlarge the noise effect and may also obviously degrade the control performance. Fortunately, above issue can be effectively settled by reducing the control gain $\bar{\mathbf{m}}$ or using extra low-pass filters [40]–[47].

Finally, using the TDE technique (14) and our designed AITSM control scheme (11)(12), we propose the following TDE-based AITSM control as

$$\begin{aligned}\boldsymbol{\tau} &= \bar{\mathbf{m}}\mathbf{u} + \boldsymbol{\tau}(t-\eta) - \bar{\mathbf{m}}\ddot{\mathbf{q}}(t-\eta)\\ \mathbf{u} &= \ddot{\mathbf{q}}_d + \boldsymbol{\psi}\left(\mathbf{e}, \hat{\mathbf{k}}\right) + \boldsymbol{\rho}_1\mathbf{s} + \boldsymbol{\rho}_2\mathbf{sig}(\mathbf{s})^{\lambda} + \hat{\rho}_3\mathbf{sgn}(\mathbf{s})\end{aligned} \tag{15}$$

where $\boldsymbol{\psi}\left(\mathbf{e}, \hat{\mathbf{k}}\right)$ is given in (12). Due to the utilization of TDE technique, our proposed control scheme requires no system dynamics and is obviously model-free. This feature will be very useful for practical applications since the accurate dynamic model can be very difficult and time-consuming to obtain. In the meantime, high control performance can also be effectively ensured with the proposed AITSM control scheme. The proposed control scheme is shown in Fig. 1 and corresponding stability analysis is given in the appendix.

C. COMPARISONS WITH EXISTING CONTROL

Our proposed TDE-based AITSM control scheme is mainly inspired by the one given in [52] as

$$\boldsymbol{\tau} = \boldsymbol{\varphi}^{-1}\left(\ddot{\mathbf{q}}_d + \boldsymbol{\alpha}\dot{\mathbf{e}}^{\gamma_1} + \boldsymbol{\beta}\mathbf{e}^{\gamma_2} - \mathbf{f} + \lambda\mathbf{s} + \boldsymbol{\psi}^T\hat{\mathbf{A}}\frac{\mathbf{s}}{\|\mathbf{s}\|}\right) \tag{16}$$

$$\dot{\hat{\mathbf{A}}} = \boldsymbol{\Gamma}\boldsymbol{\psi}\chi(\mathbf{s}), \quad \chi(\mathbf{s}) = \begin{cases}\|\mathbf{s}\| + \mu & \text{if } \|\mathbf{s}\| \neq 0\\ 0 & \text{if } \|\mathbf{s}\| = 0\end{cases} \tag{17}$$

with the ITSM manifold designed as

$$\mathbf{s} = \dot{\mathbf{e}} + \int_0^t \left(\boldsymbol{\alpha}\dot{\mathbf{e}}^{\gamma_1} + \boldsymbol{\beta}\mathbf{e}^{\gamma_2}\right)\mathbf{d}t \tag{18}$$

where $\boldsymbol{\alpha}$, $\boldsymbol{\beta}$, γ_1 and γ_2 are the same control gains with our proposed control scheme, while $\boldsymbol{\varphi}$ and $\mathbf{f}$ stand for the system dynamic information, and λ and μ are positive gains. For more detailed information concerning above control, please refer to [52]. It should be noted that the fractional power γ_1 and γ_2 may lead to $\dot{\mathbf{e}}^{\gamma_1} \notin \mathbf{R}, \mathbf{e}^{\gamma_2} \notin \mathbf{R}$ when $e_i < 0$ and $\dot{e}_i < 0$. Thus, we have used $\mathbf{sig}(x)^y$ in our proposed control scheme to avoid this issue. Additionally, $\mathbf{sig}(x)^y$ is also used for (16)-(18) in the forthcoming experimental studies.

It can be observed clearly from (16) that the existing control requires system dynamics; meanwhile our newly proposed one is model-free. Thus, our control scheme will be more suitable for practical applications than the existing one since it is usually quite difficult to obtain the exact dynamic model. More importantly, our proposed control has obvious advantages in the following two aspects.

1) Adaptive law: taking the adaptive law (17) to analyze, we can see that the adaptive speed is non-negative, which means the control gain can only increase and will not decrease under all situations. This may lead to improper large control gain under long-time process, and then serious chattering will occur. For comparisons, our newly proposed adaptive algorithm can properly adjust the control gain timely and accurately. As explained aforesaid, our adaptive law will increase the gain when the control accuracy is not satisfactory and decrease it rapidly when the control performance is relative good. Thanks to this adaptive mechanism, the

control performance is further enhanced and potential chattering issue can also be successfully suppressed.

2) AITSM control scheme: comparing the sliding mode manifolds (6) and (18), we can easily see that the existing one (18) uses constant gains. In the meantime, our newly proposed one (6) brings in an adaptive gain to further enhance the control performance. Thanks to the application of adaptive gain, the AITSM manifold can still provide good comprehensive performance under complex lumped disturbance. For the reaching law part, the existing control uses $\boldsymbol{\psi}^T\hat{\mathbf{A}}\mathbf{s}/\|\mathbf{s}\|$ with a monotonically increasing gain $\hat{\mathbf{A}}$. To effectively handle all the uncertainties, the gain $\hat{\mathbf{A}}$ will be relative large and may lead to serious chatters considering its monotonically increasing feature. For comparisons, our reaching law combines the FTSM reaching law with the adaptive part $\hat{\boldsymbol{\rho}}_3\mathbf{sgn}(\mathbf{s})$. The FTSM reaching law is used as a basic framework to handle the relative slow time-varying uncertainties, while the $\hat{\boldsymbol{\rho}}_3\mathbf{sgn}(\mathbf{s})$ is applied to handle the fast time-varying uncertainties. Benefiting from the adoption of FTSM reaching law part, the adaptive gain $\hat{\boldsymbol{\rho}}_3$ is reduced and the potential chatters will be effectively eased. Then, better comprehensive control performance can be ensured with our newly proposed control scheme.

Above claims will be verified through comparative experiments in the following section.

Remark 1: It may be unfair to compare our proposed control with the one from [52] in the aspect of whether they require system dynamics or not. Due to the utilization of TDE technique, our proposed control is model-free and easy to use in practical applications. Therefore, to highlight our contributions in AITSM scheme and guarantee fair comparisons, we have also applied the TDE technique to the control from [52] in the following experimental studies.

D. CONTROL GAINS TUNING PROCEDURES

To effectively apply our proposed control scheme, the control gains should be suitably tuned. The delayed time η can be easily determined by selected as one or several sampling periods. Then, the following tuning procedures will be briefly given based on the ones reported in [47].

1) Set $\boldsymbol{\mu}_1 = \boldsymbol{\mu}_2 = \boldsymbol{\rho}_1 = \boldsymbol{\rho}_2 = \boldsymbol{\theta} = \mathbf{k}_3 = \mathbf{0}$, $\boldsymbol{\alpha} = \boldsymbol{\beta} = \mathbf{k}_1 = \mathbf{1}_n$, tune γ_1 by reducing itself from 1 and calculate γ_2 with $\gamma_2 = \gamma_1/(2-\gamma_1)$, while checking the control performance; tune $\bar{\mathbf{m}}$ by increasing itself from small value to large one until the control performance tend to degrade;
2) Maintain $\boldsymbol{\mu}_1 = \boldsymbol{\mu}_2 = \boldsymbol{\rho}_1 = \boldsymbol{\rho}_2 = \boldsymbol{\theta} = \mathbf{k}_3 = \mathbf{0}$, $\boldsymbol{\alpha} = \boldsymbol{\beta} = \mathbf{1}_n$, tune $\mathbf{k}_1$ by increasing itself from small value while checking the control performance; then, $\boldsymbol{\alpha}$, $\boldsymbol{\beta}$, $\mathbf{k}_3$, $\boldsymbol{\rho}_1$, $\boldsymbol{\rho}_2$ can be tuned using the same procedure;
3) Maintain $\boldsymbol{\mu}_1 = \boldsymbol{\mu}_2 = \mathbf{0}$, $\mathbf{k}_2 = \mathbf{k}_4 = \mathbf{1}_n$ and set $\boldsymbol{\theta} = \boldsymbol{\theta}_{\max}$, then tune $\boldsymbol{\theta}_{\max}$ by increasing itself from $\mathbf{0}$ while checking the control performance;
4) Maintain $\boldsymbol{\mu}_1 = \boldsymbol{\mu}_2 = \mathbf{k}_2 = \mathbf{k}_4 = \mathbf{1}_n$, tune $\boldsymbol{\Delta}$ according to the amplitude of sliding variable $\mathbf{s}$; then, tune $\boldsymbol{\mu}_1$ and $\boldsymbol{\mu}_2$ by increasing themselves from small values while checking the control performance; afterwards, $\mathbf{k}_2$ and $\mathbf{k}_4$ can be regulated using the same way;
5) Repeat 1)-4) or partial of them when the control performance does not reach the desired level.

Remark 2: It should be noted that the order of above procedures can be properly regulated according to the practical performance of the control system.

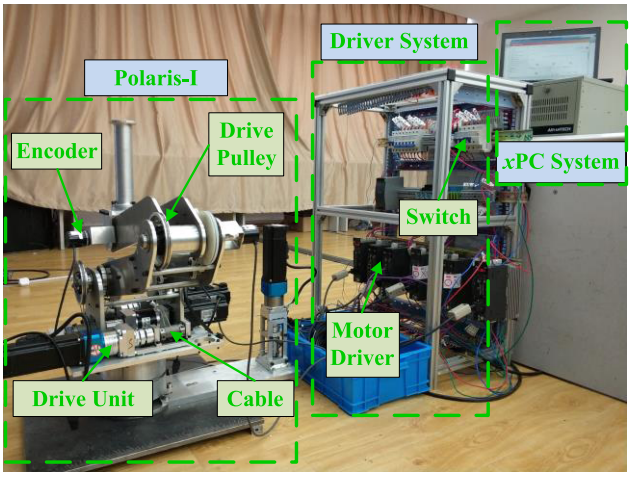

FIGURE 2. The overall control system for Polaris-I.

IV. EXPERIMENTS

To demonstrate the effectiveness and superiorities of our newly proposed TDE-based AITSM control scheme over the existing method, two comparative experiments were conducted using a newly developed cable-driven manipulator named "Polaris-I".

A. SYSTEM DESCRIPTION

The overall control system for Polaris-I is presented in Fig. 2. We can observe from Fig. 2 that all the drive motors and their reducers are arranged in the base instead of the joints.

This design can effectively reduce the moving inertial and bring much safer interactions with human. The motors are Delta ECMA-CA0604SS and their drivers are ASD-A2- 042-L. The motors have rated torque and speed of 1.27 N · m and 3000rpm. The adopted encoders are E6B2-CWZ1X 2000P/R, which have resolution of 0.045°. Mean-while, both planetary and cable reducers are applied in Polaris-I with reduction ratios of 1:10 and 1:3.3, respecttively. To execute the control algorithms, we use the x PC system with a PCI-6229 board from National Instrument. The sampling time is chosen as 1ms in the following comparative experiments.

Two comparative experiments were conducted with our newly proposed TDE-based AITSM control scheme and the one from [52]. For simplicity, the one from [52] will be referred as Controller 2 in what follows. Note that the AITSM control reported in [52] is a model-based one, while the dynamic model for Polaris-I has not been accurately

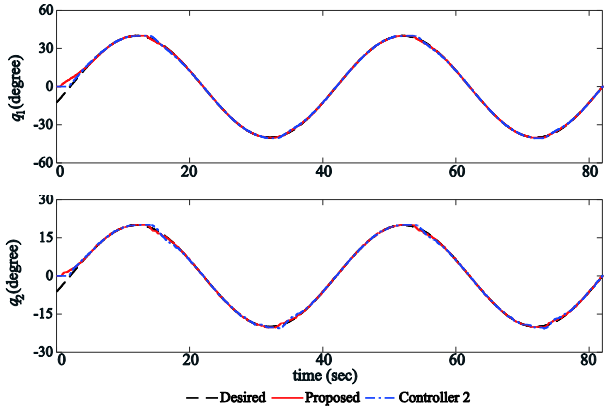

FIGURE 3. Scenario one: control performance of joint 1 and 2 under T = 40s.

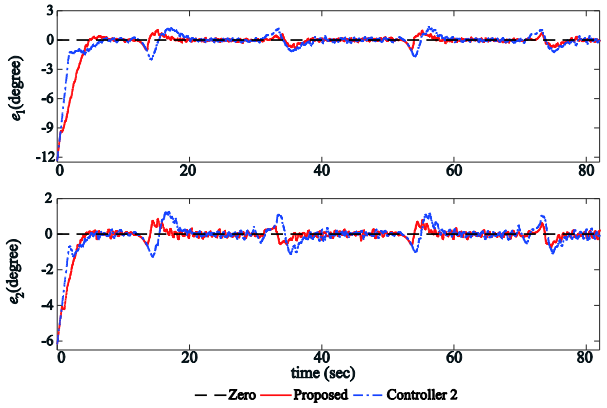

FIGURE 4. Scenario one: control errors of joint 1 and 2 under T = 40s.

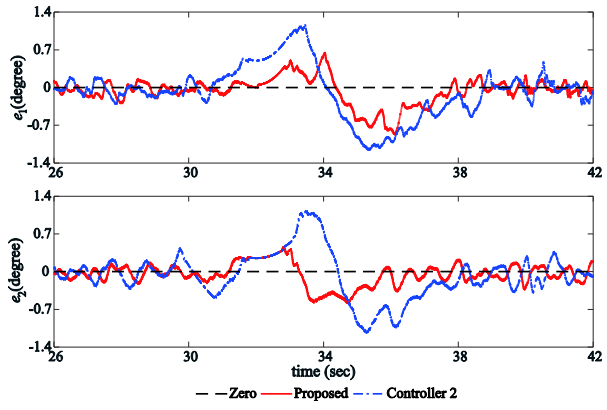

FIGURE 5. Scenario one: control errors of joint 1 and 2 in peak phase under $T = 40$s.

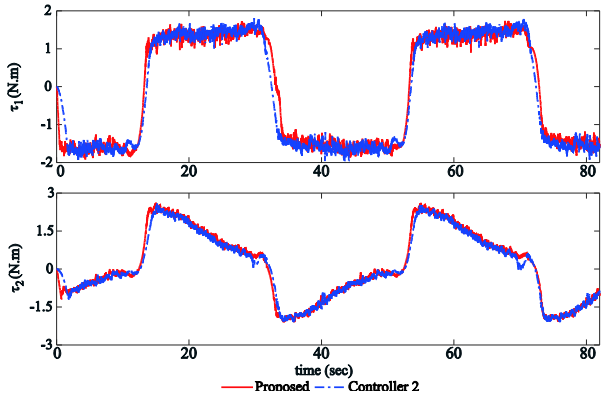

FIGURE 6. Scenario one: control efforts of joint 1 and 2 under $T = 40$s.

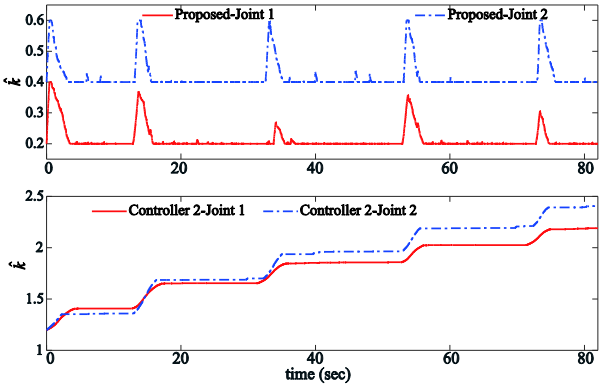

FIGURE 7. Scenario one: adaptive gain $\hat{\mathbf{k}}$ of joint 1 and 2 under $T = 40$s.

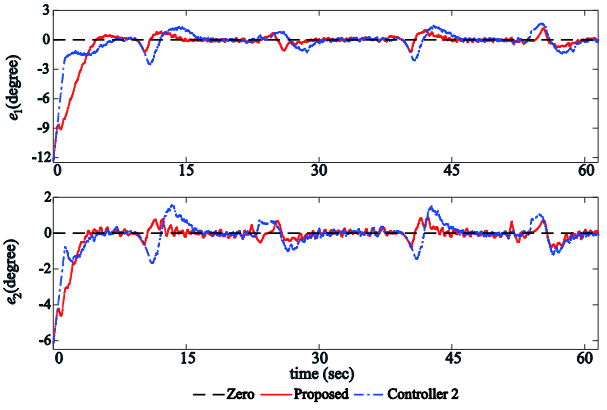

FIGURE 8. Scenario one: control errors of joint 1 and 2 under $T = 30$s.

obtained yet. Therefore, we also applied TDE technique to Controller 2 for fairness. Afterwards, it can be easily achieved by set $\hat{\mathbf{k}}$ to a constant $\mathbf{k}$, and replace the ARL with (17). In experiment one, both control schemes are utilized to track a sinusoidal reference trajectory with a non-zero initial position. Three different periods are used for the sinusoidal reference trajectory to efficiently demonstrate the performance of both control schemes. Afterwards, 0.5kg load was added into the end effector of Polaris-I to demonstrate the robustness of our newly proposed control scheme under unknown uncertainties.

Then, the control parameters for our newly proposed control scheme were selected as $\boldsymbol{\alpha} = \text{diag}(2,2)$, $\boldsymbol{\beta} = \text{diag}(1,2)$, $\gamma_1 = 0.8$, $\gamma_2 = \gamma_1/(2-\gamma_1)$, $\boldsymbol{\rho}_1 = \text{diag}(1.8,\ 1.2)$, $\boldsymbol{\rho}_2 = \text{diag}(0.35,\ 0.25)$, $\lambda = 0.8$, $\boldsymbol{\mu}_1 = \text{diag}\ (4.5,\ 9)$, $\boldsymbol{\mu}_2 = \text{diag}\ (9,\ 12)$, $\boldsymbol{\theta}_{\max} = \text{diag}(0.2,\ 0.2)$, $\Delta = 0.01 \times$

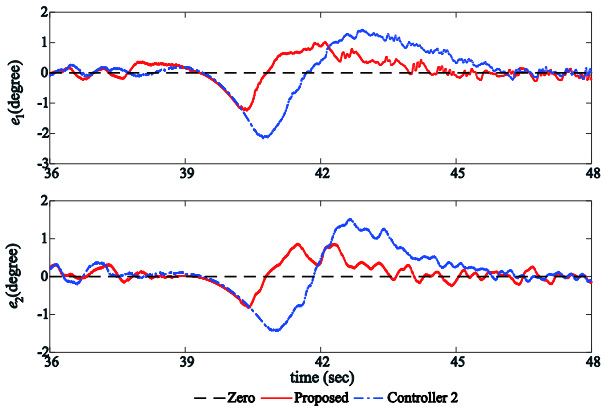

FIGURE 9. Scenario one: control errors of joint 1 and 2 in peak phase under $T = 30$s.

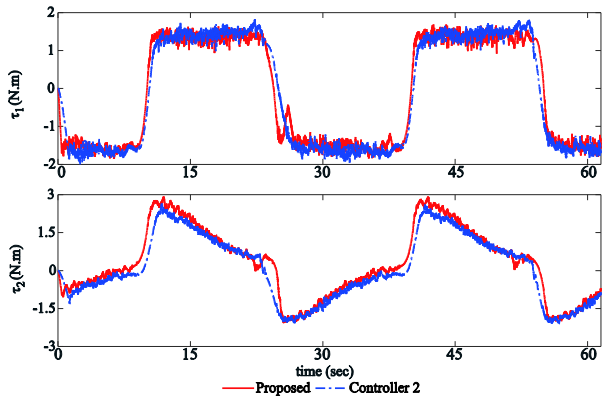

FIGURE 10. Scenario one: control efforts of joint 1 and 2 under $T = 30$s.

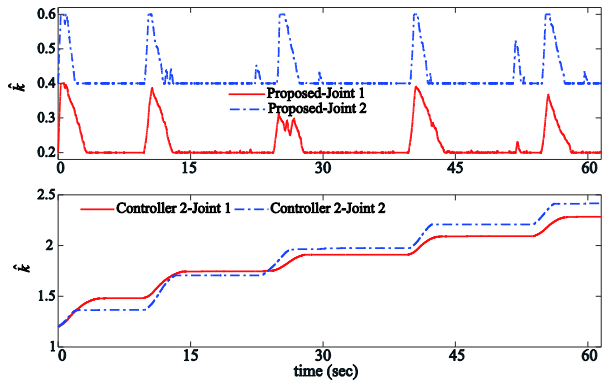

FIGURE 11. Scenario one: adaptive gain $\hat{\mathbf{k}}$ of joint 1 and 2 under $T = 30$s.

diag(2.5, 3), $\mathbf{k}_1$ = diag(0.2, 0.4), $\mathbf{k}_2$ = diag(5, 2.5), $\mathbf{k}_3$ = diag(0.5, 0.5), $\mathbf{k}_4$ = diag(1, 1), $\bar{\mathbf{m}}$ = 0.01 × diag(1.2, 1.2), η = 2 ms, and the initial value of θ is set to zero. In practical applications, the term $\mathbf{sgn}(\mathbf{s})$ for our control scheme and (16) may result in serious chattering problem. Thus, we used a saturation function to settle this issue with a boundary as 0.01 × (6, 6). The parameters for Controller 2 were selected exactly the same with ours, except that

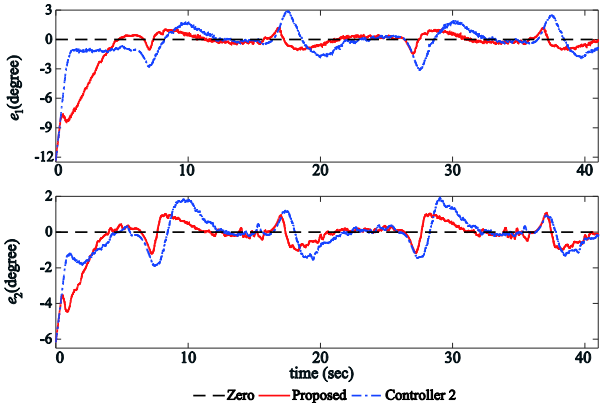

FIGURE 12. Scenario one: control errors of joint 1 and 2 under T = 20s.

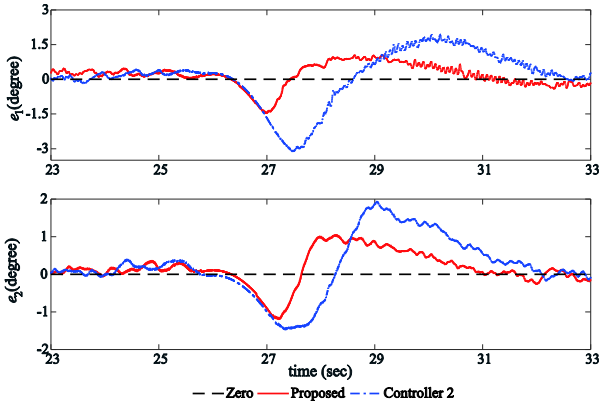

FIGURE 13. Scenario one: control errors of joint 1 and 2 in peak phase under T = 20s.

TABLE 1. RMSE values of steady control errors.

(degree / period)	T=40 s	T=30 s	T=20 s
Proposed joint 1	0.26	0.36	0.53
Controller 2 joint 1	0.47	0.67	1.08
Proposed joint 2	0.22	0.29	0.46
Controller 2 joint 2	0.36	0.50	0.69

$\boldsymbol{\mu}$ = diag(0.02, 0.1), Δ = 0.01 × diag(3.5,4) and the initial of $\boldsymbol{\theta}$ is set to $\boldsymbol{\theta}$ = diag(4, 3).

B. EXPERIMENTAL RESULTS

1) SCENARIO ONE

In this scenario, Polaris-I will be controlled to track a sinusoidal reference trajectory with three different periods. This experiment will efficiently show the control performance comparisons of our proposed control and Controller 2. Additionally, we calculated the root-mean-squared error (RMSE) and Maximum error (MAXE) using the experimental data from the second period. The RMSE and MAXE are used to analyze the steady control performance quantitatively under three different periods. Finally, the experimental results for scenario one are given in Fig. 3-15, Table 1 and 2.

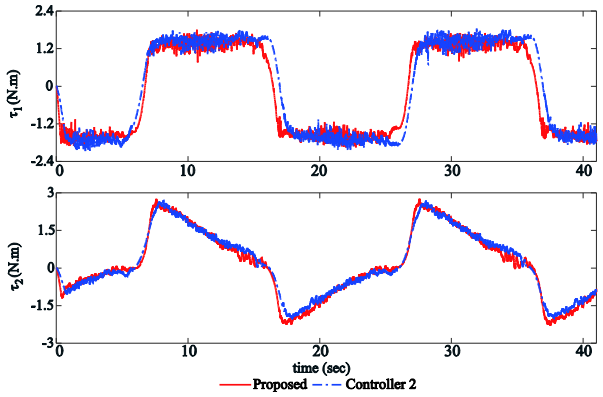

FIGURE 14. Scenario one: control efforts of joint 1 and 2 under T = 20s.

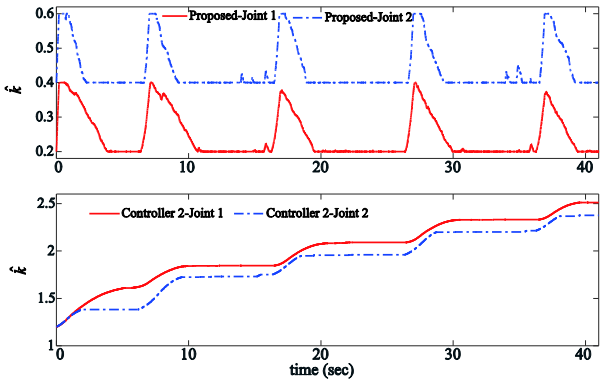

FIGURE 15. Scenario one: adaptive gain $\hat{\mathbf{k}}$ of joint 1 and 2 under T = 20s.

TABLE 2. MAXE values of steady control errors.

(degree / period)	T=40 s	T=30 s	T=20 s
Proposed joint 1	1.03	1.25	1.47
Controller 2 joint 1	1.71	2.17	3.13
Proposed joint 2	0.82	0.87	1.20
Controller 2 joint 2	1.18	1.53	1.94

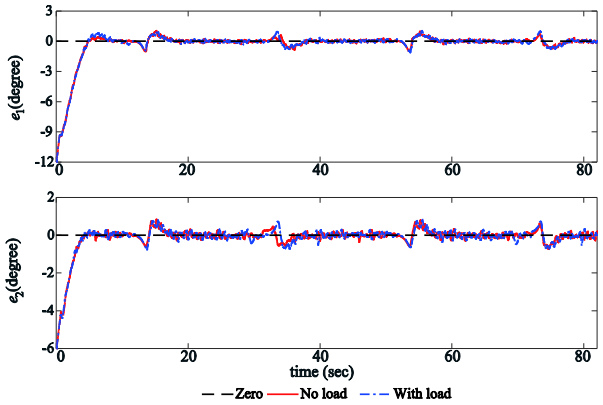

FIGURE 16. Scenario two: control errors of joint 1 and 2 with 0.5kg load.

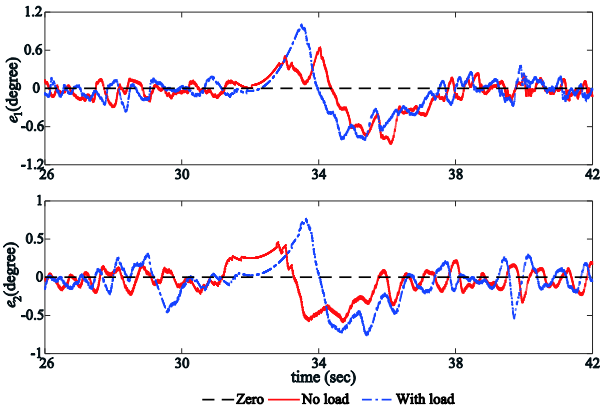

FIGURE 17. Scenario two: control errors of joint 1 and 2 in peak phase with 0.5kg load.

As shown in Fig. 3-15, both control schemes can provide good tracking control performance of the desired trajectory under three different periods. This result clearly verifies the effectiveness of TDE technique (14), ITSM manifold (18), AITSM manifold (6), combined ARL (8) and the adaptive law (17). High control accuracy and fast dynamical response have been clearly observed with these experimental results. Still, our newly proposed control scheme can ensure better comprehensive control performance than Controller 2 as shown in Fig. 4-5, Fig. 8-9, and Fig. 12-13. This result strongly verifies the superiorities of our newly proposed control over the existing Controller 2. Additionally, we will take Fig. 7, Fig. 11 and Fig. 15 to analyze. It can be observed clearly that our proposed adaptive algorithm will increase (decrease) $\boldsymbol{\theta}$ rapidly when the control performance is unsatisfactory (satisfactory). In the meantime, the control parameter $\boldsymbol{\theta}$ will remain small in most of the time. Above adaptive mechanism can effectively improve the control accuracy, while still suppress the noise effect and potential chattering issue stimulatingly. On the other hand, the adaptive algorithm proposed in [52] is *monotonically increasing* and may lead to improper large control gains as shown in Fig. 7, Fig. 11 and Fig. 15. The gain $\hat{\mathbf{k}}$ increases when the control performance is unsatisfactory and will remain the current value when the control performance turns satisfactory. Afterwards, the gain $\hat{\mathbf{k}}$ will increase again when the control performance tend to degrade. It is obvious that the gain $\hat{\mathbf{k}}$ may become extremely large after long time control. On the contrary, our proposed adaptive algorithm can adjust the gain $\hat{\mathbf{k}}$ timely and accurately based on the current control performance. Additionally, the utilization of FTSM reaching law in our combined ARL also reduces the gain $\hat{\mathbf{k}}$ greatly for our proposed control scheme as shown in Fig. 7, Fig. 11 and Fig. 15. This will further suppress the noise effect and potential chattering problem.

To quantitatively compare the control performance, we take the RMSE and MAXE from Table I and II to analyze. Specifically, we will analyze the results from $T = 40$s and other two cases can be analyzed using the same procedures. For RMSE, our proposed control scheme ensures 0.26° and 0.22° for joint 1 and 2, respectively. Meanwhile, Controller 2

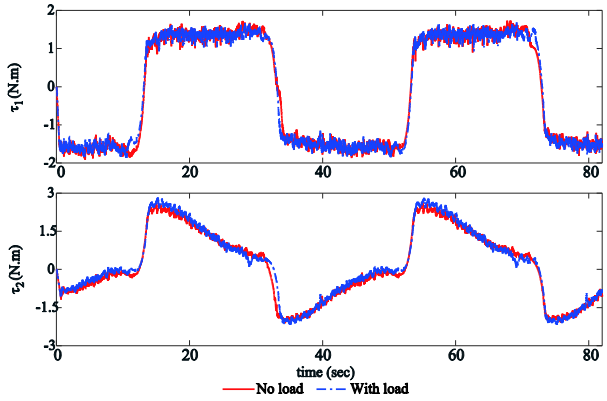

FIGURE 18. Scenario two: control efforts of joint 1 and 2 with 0.5kg load.

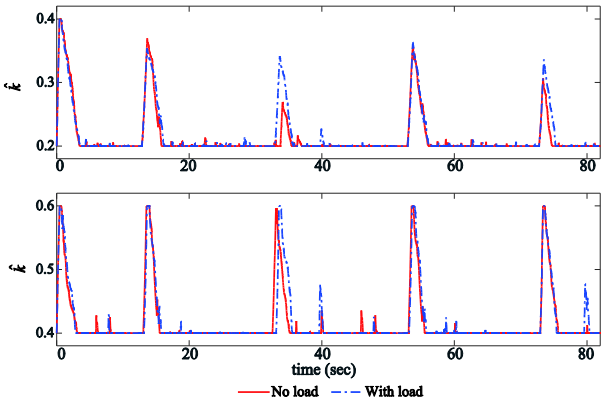

FIGURE 19. Scenario two: adaptive gain $\hat{k}$ of joint 1 and 2 with 0.5kg load.

TABLE 3. Control performance comparison between 0.5kg and no load.

(degree)	RMSE	MAXE
0.5kg load joint 1	0.29	1.16
No load joint 1	0.26	1.03
0.5kg load joint 2	0.24	0.82
No load joint 2	0.22	0.82

provides 0.47° and 0.36° for joint 1 and 2, respectively. It is obvious that our control scheme ensures 55.3% and 61.1% of the RMSE values by Controller 2. For MAXE, our proposed control scheme ensures 1.03° and 0.82° for joint 1 and 2, respectively. Meanwhile, Controller 2 pro-vides 1.71° and 1.18° for joint 1 and 2, respectively. The percentages are 60.2% and 69.5% for joint 1 and 2, respecttively. Similar results can be effectively obtained with the other two cases. It is obvious that our proposed control scheme can provide higher control accuracy than Controller 2 under all three periods, which effectively verifies the superiorities of our newly proposed AITSM manifold (6) over the existing ITSM manifold (18) from [52] and the advantages of our newly proposed adaptive law (9) over the existing one (17) from [52].

2) SCENARIO TWO

To demonstrate the robustness of our newly proposed control scheme under uncertainties, we added 0.5kg load into the end effector of Polaris-I. It should be noted that the mass of last two links are 2.5kg and 1.2kg, respectively. Then, the same reference trajectory with $T = 40$s was sent to Polaris-I. Furthermore, the RMSE and MAXE are also calculated using the experimental data from the second period. Corresponding results are given in Fig. 16-19 and Table 3.

As indicated in Fig. 16-19, our newly proposed control scheme can still guarantee satisfactory control performance under 0.5kg load. High control accuracy and fast dynamical response have been clearly observed under this situation. Meanwhile, the control performance indeed degrades a little as shown in Fig. 17. To make the comparison accurate, we will analyze Table III. For RMSE, 11.5% and 9.1% increases have been observed for joint 1 and 2, respectively. For MAXE, 12.6% and 0% increases have been obtained for joint 1 and 2, respectively. By taking the mass of last two links into consideration, we can see that strong robust-ness has been successfully guaranteed by our newly proposed control scheme.

Overall, both control schemes can provide good tracking control of the cable-driven manipulator Polaris-I. Still, better comprehensive control performance has been experimentally observed with our newly proposed control scheme compared with the existing one.

V. CONCLUSIONS

A novel TDE-based AITSM control scheme is proposed for the tracking control of cable-driven manipulators under complex lumped uncertainties in this paper. The proposed control scheme requires no system dynamics and is model-free, therefore it is suitable for complicated practical applications. Meanwhile, thanks to the utilization of the pro-posed AITSM manifold and combined ARL, the proposed control scheme can provide high control precision, fast dynamical response and strong robustness. The stability of the closed-loop control system is proved using Lyapunov stability theory. Comparative experimental results show that our newly proposed control scheme can ensure better comprehensive control performance than the existing AITSM control method.

APPENDIX
PROOF OF THE STABILITY

Lemma 1 [61]: For the following system

$$\begin{cases} \dot{x}_1 = x_2 \\ \dot{x}_2 = -k_1 sig\,(x_2)^{a_1} - k_2 sig\,(x_1)^{a_2} \end{cases} \tag{19}$$

where k_1, k_2, a_1, a_2 are positive constants satisfying $a_2 = a_1/(2 - a_1)$, $0 < a_1 < 1$. Also, they are selected such that the polynomial $r^2 + k_1 r + k_2$ is *Hurwitz*. Then, the origin of system (19) will be a globally finite-time-stable equilibrium.

For detailed proof of Lemma 1, please refer to [61].

Then, the stability of the close-loop control system will be briefly proved using the similar procedures from [61].

Substituting the control scheme (15) into the dynamic model (4), we have

$$\boldsymbol{\varepsilon} = \ddot{\mathbf{e}} + \boldsymbol{\psi}\left(\mathbf{e}, \hat{\mathbf{k}}\right) + \boldsymbol{\rho}_1 \mathbf{s} + \boldsymbol{\rho}_2 \mathbf{sig}\left(\mathbf{s}\right)^{\lambda} + \hat{\boldsymbol{\rho}}_3 \mathrm{sgn}\left(\mathbf{s}\right) \quad (20)$$

where $\boldsymbol{\varepsilon} = \bar{\mathbf{m}}^{-1}\left(\mathbf{w} - \hat{\mathbf{w}}\right)$, $|\varepsilon_i| \leq \Phi_i$ stands for the bounded TDE error which is caused by the utilization of TDE technique. Meanwhile, the boundedness proof of ε can be found in [40] and will be omitted here for concision.

For simplicity, we will analyze the ith DOF. Select the following Lyapunov candidate as

$$V = \frac{1}{2} s_i^2 + \frac{k_{3i} k_{4i}}{2\mu_{1i}} \theta_i^2 \quad (21)$$

Note that the adaptive gains $\hat{k}_{ii}$ and $\hat{\rho}_{3ii}$ are both updated using θ_i, thus above Lyapunov candidate has considered the adaptive algorithm.

Differentiating V respect to time yields

$$\begin{aligned} \dot{V} &= s_i \dot{s}_i + \frac{k_{3i} k_{4i}}{\mu_{1i}} \theta_i \dot{\theta}_i \\ &= s_i \left(\varepsilon_i - \rho_{1i} s_i - \rho_{2i} sig\left(s_i\right)^{\lambda} - \hat{\rho}_{3i} \mathrm{sgn}\left(s_i\right)\right) + \frac{k_{3i} k_{4i}}{\mu_{1i}} \theta_i \dot{\theta}_i \\ &\leq \Phi_i \left|s_i\right| - \rho_{1i} s_i^2 - \rho_{2i} \left|s_i\right|^{\lambda+1} - \hat{\rho}_{3i} \left|s_i\right| + \frac{k_{3i} k_{4i}}{\mu_{1i}} \theta_i \dot{\theta}_i \end{aligned} \quad (22)$$

Substituting the designed $\hat{\rho}_{3i}$ into (22), we have

$$\begin{aligned} \dot{V} \leq -\rho_{1i} s_i^2 - \rho_{2i} \left|s_i\right|^{\lambda+1} - k_{3i}\left(1 + k_{4i}\theta_i\right)\left|s_i\right| \\ + \Phi_i \left|s_i\right| + \frac{k_{3i} k_{4i}}{\mu_{1i}} \theta_i \dot{\theta}_i \end{aligned} \quad (23)$$

Afterwards, we will take the adaptive algorithm (9) into consideration. Two cases will be analyzed.

When $\dot{\theta}_i \leq 0$ holds, i.e. $\dot{\theta}_i = -\mu_{1i}\left|s_i\right|$ or $\dot{\theta}_i = -\mu_{2i}\left|s_i\right|$, we have $\frac{k_{3i} k_{4i}}{\mu_{1i}} \theta_i \dot{\theta}_i \leq 0$. Therefore, (23) can be further given as

$$\dot{V} \leq -\rho_{1i} s_i^2 - \rho_{2i} \left|s_i\right|^{\lambda+1} - k_{3i} \left|s_i\right| - k_{3i} k_{4i} \theta_i \left|s_i\right| + \Phi_i \left|s_i\right| \quad (24)$$

When $\dot{\theta}_i > 0$ holds, i.e. $\dot{\theta}_i = \mu_{1i}\left|s_i\right|$, (23) can be given as

$$\dot{V} \leq -\rho_{1i} s_i^2 - \rho_{2i} \left|s_i\right|^{\lambda+1} - k_{3i} \left|s_i\right| + \Phi_i \left|s_i\right| \quad (25)$$

Comparing (24) and (25), we can see that (25) is a stricter condition than (24). Thus, we will analyze (25) afterwards.

Properly select the gain k_{3i} such that $k_{3i} \geq \Phi_i$, we have

$$\dot{V} \leq -\rho_{1i} s_i^2 - \rho_{2i} \left|s_i\right|^{\lambda+1} \quad (26)$$

It should be noted that the TDE error is usually extremely small due to the small delayed time η. Thus, the condition $k_{3i} \geq \Phi_i$ can be easily fulfilled.

It can be observed from (26) that $\dot{V}$ will be continuously decreasing until we have $s_i = \dot{s}_i = 0$. Afterwards, (6) can be re-written as

$$\dot{e}_i + \hat{k}_{ii} \alpha_{ii} sig\left(\dot{e}_i\right)^{\gamma_1} + \hat{k}_{ii} \beta_{ii} sig\left(e_i\right)^{\gamma_2} = 0 \quad (27)$$

Then, based on Lemma 1, (27) will be globally finite-time-stable. Finally, the stability of the closed-loop control system is proved.

REFERENCES

[1] Y. Wang, L. Gu, Y. Xu, and X. Cao, "Practical tracking control of robot manipulators with continuous fractional-order nonsingular terminal sliding mode," *IEEE Trans. Ind. Electron.*, vol. 63, no. 10, pp. 6194–6204, Oct. 2016.

[2] Y. Wang, L. Gu, B. Chen, and H. Wu, "A new discrete time delay control of hydraulic manipulators," *Proc. Inst. Mech. Eng. I, J. Syst. Control Eng.*, vol. 231, no. 3, pp. 168–177, Mar. 2017.

[3] T. X. Dinh, T. D. Thien, T. H. V. Anh, and K. K. Ahn, "Disturbance observer based finite time trajectory tracking control for a 3 DOF hydraulic manipulator including actuator dynamics," *IEEE Access*, vol. 6, pp. 36798–36809, 2018.

[4] W. Zheng and M. Chen, "Tracking control of manipulator based on high-order disturbance observer," *IEEE Access*, vol. 6, pp. 26753–26764, 2018.

[5] J. Xu, F. Zeng, Y.-H. Chen, and H. Guo, "Robust constraint following stabilization for mechanical manipulators containing uncertainty: An adaptive ϕ approach," *IEEE Access*, vol. 6, pp. 58728–58736, 2018.

[6] M. Yuan, Z. Chen, B. Yao, and X. Zhu, "Time optimal contouring control of industrial biaxial gantry: A highly efficient analytical solution of trajectory planning," *IEEE/ASME Trans. Mechatronics*, vol. 22, no. 1, pp. 247–257, Feb. 2017.

[7] W. T. Townsend, "The effect of transmission design on force-controlled manipulator performance," Ph.D. dissertation, Cambridge Artif. Intell. Lab., Mass. Inst. Technol., Cambridge, MA, USA, 1988.

[8] T. Lens and O. Stryk, "Design and dynamics model of a lightweight series elastic tendon-driven robot arm," in *Proc. IEEE Int. Conf. Robot. Automat.*, Karlsruhe, Germany, May 2013, pp. 4512–4518.

[9] Y. Wang, S. Jiang, B. Chen, and H. Wu, "A new continuous fractional-order nonsingular terminal sliding mode control for cable-driven manipulators," *Adv. Eng. Softw.*, vol. 119, pp. 21–29, May 2018.

[10] Y. Wang, F. Yan, S. Jiang, and B. Chen, "Time delay control of cable-driven manipulators with adaptive fractional-order nonsingular terminal sliding mode," *Adv. Eng. Softw.*, vol. 121, pp. 13–25, Jul. 2018.

[11] Y. Wang, S. Wang, Q. Wei, M. Tan, C. Zhou, and J. Yu, "Development of an underwater manipulator and its free-floating autonomous operation," *IEEE/ASME Trans. Mechatronics*, vol. 21, no. 2, pp. 815–824, Apr. 2016.

[12] D. Song, L. Zhang, and F. Xue, "Configuration optimization and a tension distribution algorithm for cable-driven parallel robots," *IEEE Access*, vol. 6, pp. 33928–33940, 2018.

[13] Y. Wang, F. Yan, F. Ju, B. Chen, and H. Wu, "Optimal nonsingular terminal sliding mode control of cable-driven manipulators using super-twisting algorithm and time-delay estimation," *IEEE Access*, vol. 6, pp. 61039–61049, 2018.

[14] W. B. Lim, S. H. Yeo, and G. Yang, "Optimization of tension distribution for cable-driven manipulators using tension-level index," *IEEE/ASME Trans. Mechatronics*, vol. 19, no. 2, pp. 676–683, Apr. 2014.

[15] V. Utkin, "Variable structure systems with sliding modes," *IEEE Trans. Autom. Control*, vol. AC-22, no. 2, pp. 212–222, Apr. 1977.

[16] V. I. Utkin, "Sliding mode control design principles and applications to electric drives," *IEEE Trans. Ind. Electron.*, vol. 40, no. 1, pp. 23–36, Feb. 1993.

[17] B. Jiang, C. Gao, Y. Kao, and Z. Liu, "Sliding mode control of Markovian jump systems with incomplete information on time-varying delays and transition rates," *Appl. Math. Comput.*, vol. 290, pp. 66–79, Nov. 2016.

[18] B. Jiang, Y. Kao, C. Gao, and X. Yao, "Passification of uncertain singular semi-Markovian jump systems with actuator failures via sliding mode approach," *IEEE Trans. Autom. Control*, vol. 62, no. 8, pp. 4138–4143, Aug. 2017.

[19] B. Jiang, H. R. Karimi, Y. Kao, and C. Gao, "A novel robust fuzzy integral sliding mode control for nonlinear semi-Markovian jump T–S fuzzy systems," *IEEE Trans. Fuzzy Syst.*, vol. 26, no. 6, pp. 3594–3604, Dec. 2018, doi: 10.1109/TFUZZ.2018.2838552.

[20] B. Jiang, H. R. Karimi, Y. Kao, and C. Gao, "Adaptive control of nonlinear semi-Markovian jump T–S fuzzy systems with immeasurable premise variables via sliding mode observer," *IEEE Trans. Cybern.*, to be published, doi: 10.1109/TCYB.2018.2874166.

[21] J. Li and Q. Zhang, "A linear switching function approach to sliding mode control and observation of descriptor systems," *Automatica*, vol. 95, pp. 112–121, Sep. 2018.

[22] G. P. Incremona, A. Ferrara, and L. Magni, "MPC for robot manipulators with integral sliding modes generation," *IEEE/ASME Trans. Mechatronics*, vol. 22, no. 3, pp. 1299–1307, Jul. 2017.

[23] Y. Zhu, J. Qiao, and L. Guo, "Adaptive sliding mode disturbance observer-based composite control with prescribed performance of space manipulators for target capturing," *IEEE Trans. Ind. Electron.*, vol. 66, no. 3, pp. 1973–1983, Mar. 2019.

[24] Y. Wang, L. Gu, M. Gao, and K. Zhu, "Multivariable output feedback adaptive terminal sliding mode control for underwater vehicles," *Asian J. Control*, vol. 18, no. 1, pp. 247–265, Jan. 2016.

[25] Y. Wang, F. Yan, B. Tian, L. Gu, and B. Chen, "Nonsingular terminal sliding mode control of underwater remotely operated vehicles," *Trans. Can. Soc. Mech. Eng.*, vol. 42, no. 2, pp. 105–115, May 2018.

[26] A. Baldini, L. Ciabattoni, R. Felicetti, F. Ferracuti, A. Freddi, and A. Monteriù, "Dynamic surface fault tolerant control for underwater remotely operated vehicles," *ISA Trans.*, vol. 78, pp. 10–20, Jul. 2018.

[27] G. Chen, B. Jin, and Y. Chen, "Nonsingular fast terminal sliding mode posture control for six-legged walking robots with redundant actuation," *Mechatronics*, vol. 50, pp. 1–15, Apr. 2018.

[28] R. de Rijk, M. Rushton, and A. Khajepour, "Out-of-plane vibration control of a planar cable-driven parallel robot," *IEEE/ASME Trans. Mechatronics*, vol. 23, no. 4, pp. 1684–1692, Aug. 2018.

[29] Y. Xia, K. Xu, Y. Li, G. Xu, and X. Xiang, "Modeling and three-layer adaptive diving control of a cable-driven underwater parallel platform," *IEEE Access*, vol. 6, pp. 24016–24034, 2018.

[30] X. Yu and Z. Man, "Multi-input uncertain linear systems with terminal sliding-mode control," *Automatica*, vol. 34, no. 3, pp. 389–392, 1998.

[31] Y. Feng, X. Yu, and Z. Man, "Non-singular terminal sliding mode control of rigid manipulators," *Automatica*, vol. 38, no. 12, pp. 2159–2167, 2002.

[32] S. Yu, X. Yu, B. Shirinzadeh, and Z. Man, "Continuous finite-time control for robotic manipulators with terminal sliding mode," *Automatica*, vol. 41, no. 11, pp. 1957–1964, Nov. 2005.

[33] K. Lu and Y. Xia, "Adaptive attitude tracking control for rigid spacecraft with finite-time convergence," *Automatica*, vol. 49, no. 12, pp. 3591–3599, 2013.

[34] Z. Yang, D. Zhang, X. Sun, W. Sun, and L. Chen, "Nonsingular fast terminal sliding mode control for a bearingless induction motor," *IEEE Access*, vol. 5, pp. 16656–16664, Sep. 2017.

[35] H. Gui and G. Vukovich, "Adaptive fault-tolerant spacecraft attitude control using a novel integral terminal sliding mode," *Int. J. Robust Nonlinear Control*, vol. 27, no. 16, pp. 3174–3196, Nov. 2017.

[36] R. Ma, G. Zhang, and O. Krause, "Fast terminal sliding-mode finite-time tracking control with differential evolution optimization algorithm using integral chain differentiator in uncertain nonlinear systems," *Int. J. Robust Nonlinear Control*, vol. 28, no. 2, pp. 625–639, Jan. 2018.

[37] G. Shen, Y. Xia, J. Zhang, and B. Cui, "Finite-time trajectory tracking control for entry guidance," *Int. J. Robust Nonlinear Control*, vol. 28, no. 18, pp. 5895–5914, Dec. 2018.

[38] T. C. S. Hsia, "A new technique for robust control of servo systems," *IEEE Trans. Ind. Electron.*, vol. 36, no. 1, pp. 1–7, Feb. 1989.

[39] K. Youcef-Toumi and O. Ito, "A time delay controller for systems with unknown dynamics," *ASME J. Dyn. Syst. Meas. Control*, vol. 112, no. 1, pp. 133–142, 1990.

[40] M. Jin, J. Lee, P. H. Chang, and C. Choi, "Practical nonsingular terminal sliding-mode control of robot manipulators for high-accuracy tracking control," *IEEE Trans. Ind. Electron.*, vol. 56, no. 9, pp. 3593–3601, Sep. 2009.

[41] Y. Wang, B. Chen, and H. Wu, "Practical continuous fractional-order nonsingular terminal sliding mode control of underwater hydraulic manipulators with valve deadband compensators," *Proc. Inst. Mech. Eng. M, J. Eng. Maritime Environ.*, vol. 232, no. 4, pp. 459–469, Feb. 2018.

[42] Y. Wang, S. Jiang, B. Chen, and H. Wu, "Trajectory tracking control of underwater vehicle-manipulator system using discrete time delay estimation," *IEEE Access*, vol. 5, pp. 7435–7443, 2017.

[43] Y. Wang, B. Chen, and H. Wu, "Joint space tracking control of underwater vehicle-manipulator systems using continuous nonsingular fast terminal sliding mode," *Proc. Inst. Mech. Eng. M, J. Eng. Maritime Environ.*, vol. 232, no. 4, pp. 448–458, Oct. 2018.

[44] Y. Wang, G. Luo, L. Gu, and X. Li, "Fractional-order nonsingular terminal sliding mode control of hydraulic manipulators using time delay estimation," *J. Vib. Control*, vol. 22, no. 19, pp. 3998–4011, 2016.

[45] M. Jin, S. H. Kang, P. H. Chang, and J. Lee, "Robust control of robot manipulators using inclusive and enhanced time delay control," *IEEE/ASME Trans. Mechatronics*, vol. 22, no. 5, pp. 2141–2152, Oct. 2017.

[46] J. Baek, S. Cho, and S. Han, "Practical time-delay control with adaptive gains for trajectory tracking of robot manipulators," *IEEE Trans. Ind. Electron.*, vol. 65, no. 7, pp. 5682–5692, Jul. 2018.

[47] Y. Wang, F. Yan, J. Chen, F. Ju, and B. Chen, "A new adaptive time-delay control scheme for cable-driven manipulators," *IEEE Trans. Ind. Informat.*, to be published, doi: 10.1109/TII.2018.2876605.

[48] J. Baek, W. Kwon, B. Kim, and S. Han, "A widely-adaptive time-delay control and its application to robot manipulators," *IEEE Trans. Ind. Electron.*, to be published, doi: 10.1109/TIE.2018.2869347.

[49] M. Jin, J. Lee, and N. G. Tsagarakis, "Model-free robust adaptive control of humanoid robots with flexible joints," *IEEE Trans. Ind. Electron.*, vol. 64, no. 2, pp. 1706–1715, Feb. 2017.

[50] S. Han, H. Wang, and Y. Tian, "Model-free based adaptive nonsingular fast terminal sliding mode control with time-delay estimation for a 12 DOF multi-functional lower limb exoskeleton," *Adv. Eng. Softw.*, vol. 119, pp. 38–47, May 2018.

[51] X. Zhang, H. Wang, Y. Tian, L. Peyrodie, and X. Wang, "Model-free based neural network control with time-delay estimation for lower extremity exoskeleton," *Neurocomputing*, vol. 272, pp. 178–188, Jan. 2018.

[52] A. Riani, T. Madani, A. Benallegue, and K. Djouani, "Adaptive integral terminal sliding mode control for upper-limb rehabilitation exoskeleton," *Control Eng. Pract.*, vol. 75, pp. 108–117, Jun. 2018.

[53] D. Zhai, A. Lu, J. Dong, and Q. Zhang, "Switched adaptive fuzzy tracking control for a class of switched nonlinear systems under arbitrary switching," *IEEE Trans. Fuzzy Syst.*, vol. 26, no. 2, pp. 585–597, Apr. 2018.

[54] D. Zhai, A.-Y. Lu, J. Dong, and Q. Zhang, "Adaptive tracking control for a class of switched nonlinear systems under asynchronous switching," *IEEE Trans. Fuzzy Syst.*, vol. 26, no. 3, pp. 1245–1256, Jun. 2018.

[55] W. Deng, J. Yao, and D. Ma, "Robust adaptive precision motion control of hydraulic actuators with valve dead-zone compensation," *ISA Trans.*, vol. 70, pp. 269–278, Sep. 2017.

[56] J. Li and Q. Zhang, "Fuzzy reduced-order compensator-based stabilization for interconnected descriptor systems via integral sliding modes," *IEEE Trans. Syst., Man, Cybern. Syst.*, to be published, doi: 10.1109/TSMC.2017.2707499.

[57] J. Li, Q. Zhang, X.-G. Yan, and S. K. Spurgeon, "Observer-based fuzzy integral sliding mode control for nonlinear descriptor systems," *IEEE Trans. Fuzzy Syst.*, vol. 26, no. 5, pp. 2818–2832, Oct. 2018.

[58] J. Li, Q. Zhang, X.-G. Yan, and S. K. Spurgeon, "Integral sliding mode control for Markovian jump T–S fuzzy descriptor systems based on the super-twisting algorithm," *IET Control Theory Appl.*, vol. 11, no. 8, pp. 1134–1143, May 2017.

[59] J. Li, Q. Zhang, X.-G. Yan, and S. K. Spurgeon, "Robust stabilization of T–S fuzzy stochastic descriptor systems via integral sliding modes," *IEEE Trans. Cybern.*, vol. 48, no. 9, pp. 2736–2749, Sep. 2018.

[60] Y. Pan, C. Yang, L. Pan, and H. Yu, "Integral sliding mode control: Performance, modification, and improvement," *IEEE Trans. Ind. Informat.*, vol. 14, no. 7, pp. 3087–3096, Jul. 2018.

[61] S. P. Bhat and D. S. Bernstein, "Geometric homogeneity with applications to finite-time stability," *Math. Control, Signals, Syst.*, vol. 17, no. 2, pp. 101–127, Jun. 2005.

YAOYAO WANG (M'17) received the B.S. degree in mechanical engineering from Southeast University, Nanjing, China, in 2011, and the Ph.D. degree in mechanical engineering from Zhejiang University, Hangzhou, China, in 2016.

He is currently a Lecturer with the College of Mechanical and Electrical Engineering, Nanjing University of Aeronautics and Astronautics, Nanjing. His current research interests include robust control and adaptive control of hydraulic manipulators and underwater vehicles, and the design and control of cable-driven manipulators.

FEI YAN received the B.S. degree in mechanical and electrical engineering from the Jiangsu University of Science and Technology, Zhenjiang, China, in 2015.

He is currently pursuing the Ph.D. degree with the College of Mechanical and Electrical Engineering, Nanjing University of Aeronautics and Astronautics, Nanjing, China. His current research interests include artificial bee colony algorithm, and design and control of cable-driven manipulators.

KANGWU ZHU received the B.S. degree from the Harbin Institute of Technology, Harbin, China, in 2005, the M.S. degree from the China Ship Scientific Research Center, Wuxi, China, in 2008, and the Ph.D. degree from Zhejiang University, Hangzhou, China, in 2012. He is currently an Associate Researcher with the Shanghai Institute of Spaceflight Control Technology, Shanghai, China. His research interests include sliding mode control and nonlinear system control.

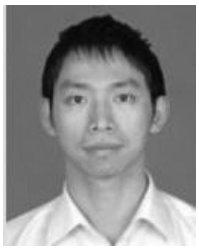

BAI CHEN received the B.S. and Ph.D. degrees in mechanical engineering from Zhejiang University, Hangzhou, China, in 2000 and 2005, respectively.

He is currently a Professor and the Ph.D. Supervisor with the College of Mechanical and Electrical Engineering, Nanjing University of Aeronautics and Astronautics, Nanjing, China. His current research interests include the design and control of surgical robots, cable-driven robots, and sperm-like swimming micro robots.

HONGTAO WU received the B.S. degree in mechanical engineering from the Northeast Heavy Machinery Institute, Tsitsihar, China, in 1982, and the M.S. and Ph.D. degrees in mechanical engineering from Tianjin University, Tianjin, China, in 1985 and 1992, respectively. Since 1998, he has been a Professor with the Nanjing University of Aeronautics and Astronautics, where he teaches the courses of Introduction to Robotics and Computational Multibody System Dynamics. He has presided over a number of the National Research Projects of China. His research interests include multibody system dynamics, robotics, parallel mechanisms, and punching machines.